Quantum-enhanced interferometry for axion searches

Denis Martynov and Haixing Miao
University of Birmingham, Birmingham B15 2TT, United Kingdom

(Received 21 April 2020; accepted 12 May 2020; published 26 May 2020)

We propose an experiment to search for axions and axionlike particles in the galactic halo using quantum-enhanced interferometry. This proposal is related to the previously reported ideas [W. DeRocco and A. Hook, Phys. Rev. D **98**, 035021 (2018); I. Obata, T. Fujita, and Y. Michimura, Phys. Rev. Lett. **121**, 161301 (2018); H. Liu, B. D. Elwood, M. Evans, and J. Thaler, Phys. Rev. D **100**, 023548 (2019)] but searches for axions in the mass range from 10^{-16} eV up to 10^{-8} eV using two coupled optical cavities. We also show how to apply squeezed states of light to enhance the sensitivity of the experiment similar to the gravitational-wave detectors. The proposed experiment has a potential to be further scaled up to a multi-km long detector. We show that such an instrument has a potential to set constrains of the axion-photon coupling coefficient of $\sim 10^{-18}$ GeV^{-1} for axion masses of 10^{-16} eV or detect the signal.

DOI: 10.1103/PhysRevD.101.095034

I. INTRODUCTION

The challenge of discovering dark matter particles comes from a variety of candidates and their interaction with the Standard Model. Weakly interacting massive particles were the most promising dark matter candidates over the past few decades. However, a set of ultrasensitive detectors, such as XENON [1], LUX [2], and PandaX [3] have not observed dark matter particles up to date and will reach neutrino background in the near future [4]. Furthermore, the Large Hadron Collider has placed stringent constraints on supersymmetry that provides the theoretical basis for weakly interacting massive particles [5]. Therefore, it is important to diversify dark matter searchers. In this paper, we consider axions [6] and axionlike particles [7–10] (ALPs) that are also well-motivated dark matter candidates.

Axions and ALPs are generically expected in many models of physics beyond the Standard Model [11]. These particles emerge as the Goldstone bosons of global symmetries that are broken at some high energy scale [6,12,13]. If dark matter consists of ALPs with mass m_a then its field behaves classically and can be written as [14]

$$a(t) = a_0 \sin(\Omega_a t + \delta(t)), \tag{1}$$

where the angular frequency $\Omega_a = 2\pi f_a = m_a$ in the natural units ($\hbar = c = 1$), $a_0 = \sqrt{2\rho_{\rm DM}}/m_a$ is the amplitude of the field, $\rho_{\rm DM} \approx 0.3$ GeV/cm^3 is the local density of dark matter, and $\delta(t)$ is the phase of the field. The phase remains constant for times $t \lesssim \tau_a$, where $\tau_a = Q_a/f_a$ is the coherence time of the field, $Q_a = v^{-2} \sim 10^6$ is the quality factor of the oscillating field, and v is the galactic virial velocity of the ALP dark matter [7]. Equation (1) neglects spatial variations of the field since ALPs wavelength $\lambda_a = (f_a v)^{-1} > 100$ km is significantly larger than the length of the proposed experiment for $m_a < 10^{-8}$ eV.

The Goldstone nature of ALPs manifests itself in their derivative interactions with the Standard Model [14]. In this paper, we consider an interaction of ALPs with photons parametrized by the coefficient $g_{a\gamma}$. The observable quantity is the phase difference accumulated by the left- and right-handed circularly polarized light that propagates in the presence of the ALP field for a time period τ. This phase difference is given by the equation [15]

$$\Delta\phi(t,\tau) = g_{a\gamma}[a(t) - a(t-\tau)] \tag{2}$$

and can be measured by sensitive laser interferometers [15–17]. For $\tau = 10$ nsec and $g_{a\gamma} = 10^{-10}$ GeV^{-1}, we get the amplitude of $\Delta\phi$ equal $\approx 3.2 \times 10^{-15}$ rad. This phase shift is significantly smaller compared to the ones observed by the gravitational-wave detectors, such as LIGO [18] and Virgo [19]. A typical source modulates the laser phase by $\sim 10^{-12}$–10^{-11} rad [20–22] but only lasts for a fraction of a second for ~ 30 solar mass black holes and ≈ 30 sec for neutron stars. However, dark matter signal can be accumulated during much longer timescales that are only limited by the duration of the experiment.

Recently, new configurations to search for ALPs were proposed in the literature [15–17,23–25]. Authors in [25] propose to search for axions around the free-spectral range of linear cavities while authors in [15] consider quarter-wave plates inside these resonators to search for axions at lower frequencies (below ≈ 20 kHz). Authors in [16] propose the design without the intracavity wave plates by utilizing a bow-tie cavity with two counterpropagating beams. This detector has a potential to search for axions with masses below 10^{-12} eV due to a limited bandwidth of

the optical resonator. Some schemes were proposed in the literature [26,27] to enhance the gain-bandwidth product of optical cavities but these schemes were not experimentally demonstrated yet. Authors in [17] found a different approach to increase the range of axion masses in their proposal up to 10^{-8} eV. They utilize a folded optical cavity with nondegenerate eigen P- and S-polarization modes. The frequency difference between these polarizations is tuned to a particular axion mass. By changing the frequency between P- and S-pol in the optical cavity, the authors proposed to search for ALPs with masses from 10^{-13} eV up to 10^{-8} eV for ∼10 m long interferometers.

In this paper, we further advance the studies in [15–17] and (i) propose a new optical configuration to scan for ALPs with masses from 10^{-16} eV up to 10^{-8} eV in Sec. II, (ii) show how to enhance the sensitivity of our detector with squeezed states of light [28,29], and (iii) calculate the sensitivity of the proposed detector with lengths of 2.5 m and 4 km to ALPs in Sec. III. The former length is a typical scale of a tabletop interferometer, while the later one is a scale of the gravitational-wave detectors, such as LIGO and Virgo. Once the third generation facilities, such as Einstein Telescope [30] and Cosmic Explorer [31], are built, the current facilities have a potential to search for dark matter using optical interferometers. We summarize our conclusions in Sec. IV.

II. OPTICAL LAYOUT

The proposed interferometer measures a difference in phase velocities between left- and right-handed circularly polarized light which propagates in the presence of the ALP field. This effect can be equivalently understood as a slow rotation of the polarization angle of a linearly polarized light in the ALP dark matter [17,32]. Our detector consists of two folded optical resonators: main and auxiliary cavities as shown in Fig. 1. The main optical cavity resonates a strong pump field in the horizontal polarization (P polarization) which is partially converted to the vertical polarization (S polarization) by the ALP field.

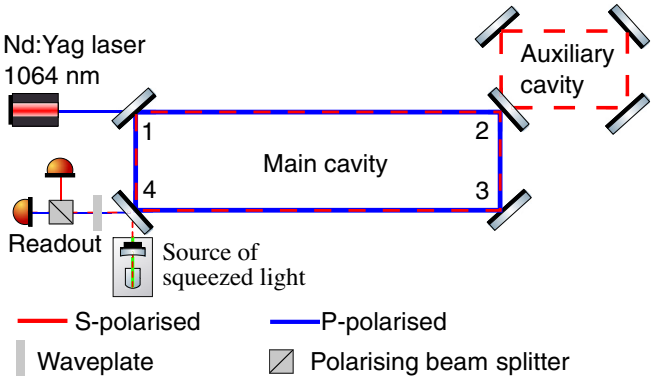

FIG. 1. Optical layout of the proposed experiment that consists of the main and auxiliary optical cavities. The mirrors in the main cavity have numbers 1 to 4 according to the discussion in the text.

The first challenge is to amplify both P- and S-polarized fields with frequencies ω_p and ω_s in the main optical cavity given that optical frequencies of these fields are separated by the ALP frequency Ω_a. Similar to [17] this challenge is solved by the folded design of the main cavity. Its two resonating modes are nondegenerate since P and S polarizations acquire different phases upon non-normal reflection from the cavity mirrors. The second challenge is to dynamically tune $\omega_p - \omega_s$ to scan for ALP masses. Authors in [17] propose to change angles of incidence of the laser beam on the cavity mirrors. Indeed, this approach will change the frequency separation between P and S polarization but can also dramatically reduce a quality factor of the optical cavity making it insensitive to the axion field. Instead of changing the angles of incidence, we propose a coupled cavity design similar to the gravitational-wave detectors. The auxiliary cavity will allow us to dynamically tune ω_s and scan over a broad range of ALP masses from 10^{-16} eV up to 10^{-8} eV by detuning the auxiliary cavity from its resonance.

In this section, we discuss how the ALPs field produces the signal in the S polarization in the main cavity, discuss how the auxiliary cavity tunes the eigenmode ω_s of the main cavity, and present the optical readout scheme.

A. Propagation of the fields in the main cavity

We now consider how linearly polarized light propagates in the ALPs field between two points separated by a distance L. We adopt Jones calculus with the electric field vector given by $(E_p, E_s)^T$, where E_p and E_s are the horizontal and vertical components of the field. The Jones matrix P for propagation of light in the ALPs field is given by the equation

$$P = A^{-1}\begin{pmatrix} e^{i\Delta\phi/2} & 0 \\ 0 & e^{-i\Delta\phi/2} \end{pmatrix} A \approx \begin{pmatrix} 1 & \Delta\phi/2 \\ -\Delta\phi/2 & 1 \end{pmatrix}, \tag{3}$$

where matrices A and A^{-1} convert electric fields from the linear to circular basis and back. In Eq. (3) we assume that $\Delta\phi \ll 1$ according to the discussion below Eq. (2). Equation (3) implies a slow rotation of the polarization angle of a linearly polarized light in the ALP field.

Phase shift $\Delta\phi$ is amplified in a high-finesse optical cavity. However, since P and S polarizations acquire a phase difference of π upon reflection from a mirror under normal angle of incidence, rotation of the polarization angle will be canceled after the round-trip propagation of the field inside the linear optical cavity [15]. Mathematically, the round-trip Jones matrix for a linear cavity is $R_1 P(t) R_2 P(t-\tau/2) \approx I$ for $f_a \ll 1/\tau$, where τ is the cavity round-trip time, $R_1 = R_2 = \left(\begin{smallmatrix} -1 & 0 \\ 0 & 1 \end{smallmatrix}\right)$ are Jones matrices

for the mirrors at normal incidence and I is a 2 by 2 identity matrix.

In order to accumulate $\Delta\phi$ over many bounces inside an optical cavity, we introduce folding in the cavity as shown in Fig. 1. Distance between mirrors 1 and 4 and mirrors 2 and 3 is significantly smaller compared to the distance between mirrors 1 and 2 and mirrors 3 and 4. Therefore, we can neglect any rotation of the polarization angle between these mirrors by the ALP field and the round-trip Jones matrix is given by the equation

$$Q = M_1 M_4 P(t) M_3 M_2 P(t - \tau/2), \tag{4}$$

where matrices M_1, M_2, M_3, M_4 correspond to reflection of the laser field from each of the four mirrors. Matrix M_2 describes reflection of the laser light from auxiliary cavity. We can express Jones matrices of the mirrors as

$$M_i = \begin{pmatrix} -1 & 0 \\ 0 & e^{i\beta_i} \end{pmatrix}, \tag{5}$$

where β_i is the phase difference accumulated by the fields in P and S polarizations during the propagation inside the optical coatings.

In general, $\beta_i \neq 0$ since reflectively of each coating layer is different for P and S polarization according to the Fresnel equations. This inequality leads to nondegenerate frequencies of the P- and S-polarized modes $\omega_p \neq \omega_s$. We propose to design stacks of the optical coating such that $e^{i(\beta_1+\beta_4)} \approx 2\pi K$ and $e^{i(\beta_2+\beta_3)} \approx 2\pi D$, where K and D are integer numbers. In this case, $M_1 M_4 = I$ and $M_2 M_3 = \left(\begin{smallmatrix} 1 & 0 \\ 0 & e^{i\beta} \end{smallmatrix}\right)$, where β is an extra phase accumulated by the S-polarized beam inside the auxiliary cavity.

B. Auxiliary cavity

We now discuss how the phase shift β is dynamically tuned by the auxiliary cavity. If phases accumulated by the fields in P and S polarizations are ξ_p and ξ_s then the reflection coefficient from the auxiliary cavity is given by the equation [33]

$$r_{p,s} = \frac{-r_2 + e^{i\xi_{p,s}}}{1 - r_2 e^{i\xi_{p,s}}}, \tag{6}$$

where r_2 is the field reflectivity of mirror 2. Figure 2 shows the argument of $r_{p,s}$ for different phases accumulated in the auxiliary cavity. We control this cavity such that $\xi_p \approx -\pi$. In this case, $r_p = -1$ even for small changes of ξ_p. S-polarized beam is close to the resonance in the auxiliary cavity $\xi_s \ll 1$ and we can write the argument of r_s as

$$\beta = \frac{4}{T_2}\xi_s, \tag{7}$$

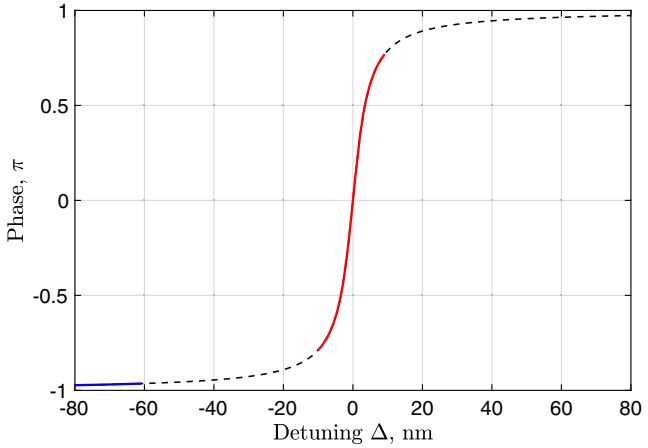

FIG. 2. Phase of the fields in P and S polarizations reflected from the auxiliary cavity. By detuning the auxiliary cavity by 20 nm, we can tune the relative phase shift between the fields in P (shown in blue) and S polarization (shown in red) by π.

where $T_2 = 1 - r_2^2$ is the power transmission of mirror 2. Small tuning of ξ_s leads to significant phase shift of the field in the S polarization in the main cavity β. This phase can be controlled using an auxiliary laser which is phase locked to the main laser [34]. We use this procedure to control the frequency of the eigenmode ω_s as discussed below.

C. Optical readout

We use Eqs. (2) and (4) to calculate the field equations for the S-polarized field in the main cavity. In the further analysis we neglect the time dependence of the pump field in the cavity $E_{p,\mathrm{cav}}$ since it is not affected by the ALP field. The field in the S polarization builds up in the main cavity due to the ALP field according to the equation

$$E_{s,\mathrm{cav}}(t) = E_{s,\mathrm{cav}}(t-\tau)e^{i\beta}\sqrt{1-T_s} - \frac{1}{2}\left[\Delta\phi\left(t, \frac{\tau}{2}\right) + \Delta\phi\left(t - \frac{\tau}{2}, \frac{\tau}{2}\right)\right] E_{p,\mathrm{cav}}, \tag{8}$$

where T_s is the power transmission of mirror 4 to the S polarization. The first term on the right-hand side of Eq. (8) represents the feedback term in the optical cavity while the second term is the excitation of the resonating field.

Equation (8) can be solved in the frequency domain. We use a Fourier transform normalized to the coherence time of the ALP field,

$$E(\Omega) = \frac{1}{\tau_a}\int_0^{\tau_a} E(t)\exp(-i\Omega t)dt, \tag{9}$$

and similar to [14] we treat the ALP phase δ from Eq. (1) as a constant over time period τ_a. Solving Eq. (8) in the frequency domain, we get the solution in the form

$$E_{s,\mathrm{cav}}(\Omega_a) = -\frac{E_{p,\mathrm{cav}}\exp(i\frac{\beta-\Omega_a\tau}{2}+\delta)}{1-\sqrt{1-T_s}\exp(i(\beta-\Omega_a\tau))}g_{a\gamma} \times\frac{\tau}{4}\mathrm{sinc}\left(\frac{\Omega_a\tau}{4}\right)\cos\left(\frac{2\beta-\Omega_a\tau}{4}\right)\sqrt{2\tau_a\rho_{\mathrm{DM}}}. \quad (10)$$

The signal field in the S polarization is measured in transmission of mirror 4 using the heterodyne readout. The field in the P polarization serves as a local oscillator in our readout scheme. First, we introduce a quarter wave plate to shift the phase between P polarization and S polarization by $\pi/2$ (see Fig. 1). The latter shift will allow us to measure the phase quadrature of the field given by Eq. (10). Then we introduce a half wave plate to convert a small fraction of the P-polarized light to S-polarized light $E_{\mathrm{LO}} = i\zeta E_{p,\mathrm{cav}}\sqrt{T_p}$, where ζ is twice the rotation angle of the half wave plate, T_p is the power transmission of mirror 4 to the P polarization. Fourier transform of the power in the S polarization at the readout port is given by equation

$$P_{\mathrm{out}}(\Omega_a) = E_{\mathrm{LO}}\sqrt{T_s}[E^*_{s,\mathrm{cav}}(-\Omega_a) - E_{s,\mathrm{cav}}(\Omega_a)], \quad (11)$$

which implies that $P_{\mathrm{out}}(\Omega_a)$ is resonantly enhanced if the following condition is satisfied:

$$\Omega_a = \pm\beta/\tau. \quad (12)$$

Therefore, the ALP mass equals the frequency separation of the P- and S-polarization eigenmodes in the main cavity that is determined by Eq. (7). Full width at half maximum of the resonance equals

$$\Delta f = \frac{T_s}{2\pi}\mathrm{FSR}, \quad (13)$$

where FSR is the free spectral range of the main cavity. Resonant amplification of the S-polarized light is schematically shown in Fig. 3.

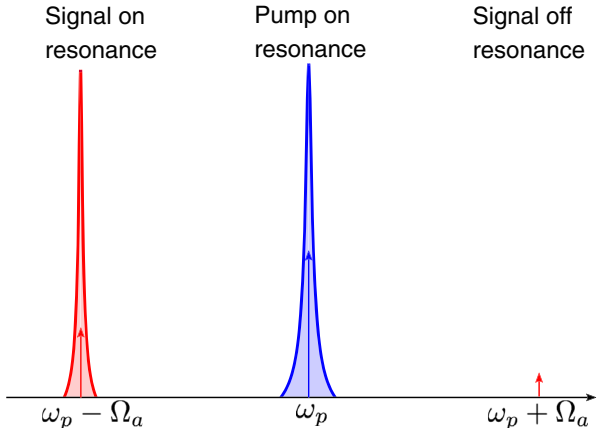

FIG. 3. ALP field converts the pump beam in the P polarization into the beam in S polarization. Both fields are resonantly enhanced in the main optical cavity.

III. SENSITIVITY

Noise sources in the laser interferometers were actively studied in the context of gravitational-wave detectors [18,19,35], optomechanical setups [36–40], and laser gyroscopes [41–45]. Gravitational-wave detectors and optomechanical setups reach fundamental shot noise at frequencies above ≈40 Hz while at lower frequencies the sensitivity degrades due to ground vibrations, thermal noises, and scattered light [46–49]. In the proposed experiment, the pump and signal fields follow the same path in the main cavity. Moreover, the mode of the auxiliary cavity has the same noise as the pump since the auxiliary cavity will be actively controlled with an auxiliary laser locking scheme [34]. Therefore, displacement noises in the main and auxiliary cavities will be canceled out in the readout. The main source of the classical noises comes from intensity fluctuations of the pump beam. These fluctuations will be measured in transmission of the polarizing beam splitter (see Fig. 1) and fed back to the laser in a high bandwidth loop. In this paper, we calculate the sensitivity of the proposed experiment above 25 mHz based on the quantum noise level.

A. Quantum squeezing

The main source of quantum noises comes from vacuum fluctuations which enter the interferometer from the readout port and through optical losses inside the cavity. Since we read out the phase quadrature of the field on the signal photodetector, the optical power due to vacuum fields b and $b^\dagger$ is given by the equation [50,51]

$$P_{\mathrm{shot}}(\Omega_a) = E_{\mathrm{LO}}[b^\dagger(-\Omega_a) - b(\Omega_a)], \quad (14)$$

where vacuum fields b and $b^\dagger$ are in the S polarization and come from the open port of the interferometer, reflect from mirror 4 and proceed to the signal photodetector. Therefore, we need to squeeze vacuum fields in the S polarization as shown in Fig. 1. Then the power spectrum density of the shot noise is given by the equation

$$|P_{\mathrm{shot}}(\Omega_a)|^2 = 2\omega_p|E_{\mathrm{LO}}|^2\exp(-2r), \quad (15)$$

where r is the squeezing factor. Modern optical tabletop experiments reach $\exp(-r)\sim 0.15$–0.5 [52–54] in the audio and radio-frequency bands and have the potential to reach a similar level of squeezing below 1 Hz. In this paper, we use $\exp(-r) = 0.3$ for the proposed experiment.

The signal-to-noise (SNR) ratio of the setup for a particular ALP mass m_a is given by [14]

$$\mathrm{SNR}^2 = \left|\frac{P_{\mathrm{out}}(\Omega_a)}{P_{\mathrm{shot}}(\Omega_a)}\right|^2\sqrt{\frac{T_{\mathrm{meas}}}{\tau_a}}, \quad (16)$$

where T_{meas} is the measurement time. The latter multiplier comes from averaging the shot noise level around

frequency Ω_a with a bandwidth of Ω_a/Q_a [14]. Equations (11) and (15) imply that $E_{\rm LO}$ cancels out in Eq. (16) and SNR does not depend on the level of the local oscillator field.

B. Integration time

We choose integration time for each ALP mass $T_{\rm meas} = N\tau_a$ according to [17,55,56]. We scan over a range of ALP masses by changing longitudinal offset of the auxiliary cavity in the range $0 \le \beta \le \pi/2$. Every step we shift the frequency difference between eigenmodes of the main cavity by its full width half maximum to keep resonance enhancement of the signal field in the S polarization. Given the total integration time of $T_{\rm int} = 1$ year, the measurement time for a particular ALP mass in units of its coherence time is given by the equation

$$N \approx \frac{\Delta f T_{\rm int}}{Q \ln({\rm FSR}/\Delta f)}, \tag{17}$$

which implies that the SNR depends on the cavity finesse for the S polarization $\mathcal{F}_s = 2\pi/T_s$ according to the equation

$${\rm SNR} \sim g_{a\gamma} N^{1/4} \sqrt{\mathcal{F}_s} \sim g_{a\gamma} \left(\frac{\mathcal{F}_s}{\ln \mathcal{F}_s}\right)^{1/4} \tag{18}$$

for $f_a > \Delta f$. In this paper, we consider $\mathcal{F}_s = 10^5$ and the latter multiplier in Eq. (18) equals ≈ 10. For $f_a < \Delta f$ the scaling of SNR with $\mathcal{F}_s$ is different from Eq. (18) since the measurement time is determined by the coherence time of ALPs with masses $\pi\Delta f$. The SNR scales according to the equation

$${\rm SNR} \sim g_{a\gamma} \left(\frac{\mathcal{F}_s^2}{\ln \mathcal{F}_s}\right)^{1/4} \tag{19}$$

for $f_a < \Delta f$ and the latter multiplier in Eq. (19) equals ≈ 170 for $\mathcal{F}_s = 10^5$.

The sensitivity of the experiment to the axion-photon coupling $g_{a\gamma}$ is shown in Fig. 4 for SNR = 1 and different lengths of the interferometer. The key property of this proposal is that the setup does not require strong magnets. Instead, ALP dark matter converts the strong optical field in one polarization into a field with an orthogonal polarization. This property implies that the current gravitational-wave facilities can host dark matter detectors in the future. Both for the tabletop 2.5 m and long-scale 4 km detectors the sensitivity curve significantly improves for $f_a < \Delta f$ since both modes $E_{s,\rm cav}(\Omega_a)$ and $E^*_{s,\rm cav}(-\Omega_a)$ resonate in the main optical cavity. These two fields interfere constructively on the signal photodetector since we measure the phase quadrature of the field. This interference explains the transition step in Fig. 4 for the tabletop experiment at $m_a \sim 10^{-12}$ eV and for the km-scale experiment at $m_a \sim 10^{-15}$ eV. Furthermore, the sensitivity of the experiment scales as $\tau_a^{-1/4} \sim m_a^{1/4}$ below Δf according to Eqs. (10) and (16) since the measurement time $T_{\rm meas}$ is the same for all frequencies smaller than Δf. This is in contrast to larger masses ($\Omega_a > 2\pi\Delta f$) since we increase the measurement time as $T_{\rm meas} = N\tau_a$ and, therefore, the sensitivity scales as $\tau_a^{-1/2} \sim m_a^{1/2}$ above Δf similar to the relation found in [17].

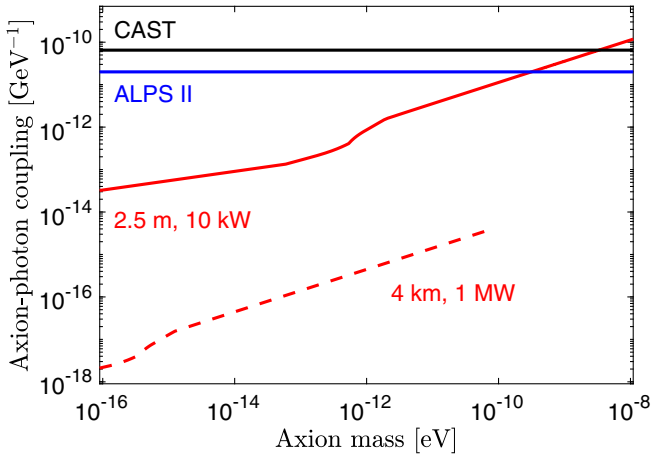

FIG. 4. Sensitivity of the proposed experiment to the axion-photon coupling coefficient after one year of integration and scanning through the ALP masses with signal-to-noise ratio of 1. We consider two optical configurations: a tabletop setup with 10 kW resonating power and a km-scale detector with 1 MW of power. The distance shown in the figure refers to the distance between mirrors 1 and 4. Existing limits from CAST [57] and design sensitivity of the ALPS II [58] detector are shown for comparison.

IV. CONCLUSIONS

We proposed a new quantum-enhanced interferometer to search for ALPs in the mass range 10^{-16} eV up to 10^{-8} eV. This mass range corresponds to frequencies of the ALP field from 25 mHz up to 2.5 MHz. In principle, the detector is sensitive at frequencies below 25 mHz but we expect that the sensitivity will be limited by technical noises rather than by quantum noises similar to the optical gyroscopes [41–45]. An experiment is needed to measure the sensitivity at these low frequencies. The upper ALP mass is limited by the free spectral range of the optical cavity and the corresponding sinc function in Eq. (10). We proposed to scan over ALP masses using an auxiliary cavity that tunes the frequency separation between the pump and signal fields in the main cavity.

We proposed a technique to enhance the quantum limited sensitivity of the interferometer by injecting squeezed states of light similar to the gravitational-wave detectors. Further steps include building a tabletop prototype which can already improve over CAST limits in the ALP mass range from 10^{-16} eV up to 10^{-9} eV. Once the technology is tested, the detector length can be scaled up. In particular,

current gravitational-wave facilities are of significant interest to this proposal.

ALP searches in the km-scale facilities have a potential to improve over the CAST limits by 5–7 orders of magnitude in the mass range 10^{-16} eV up to 10^{-10} eV or detect the signal. Current gravitational-wave facilities are ideal sites for axion interferometry since they already have vacuum envelopes and powerful lasers. New third generation gravitational-wave facilities will not only reach cosmological distances [30,31] but also create opportunities to use existing facilities for new experiments with dark matter.

ACKNOWLEDGMENTS

We thank Matthew Evans, Hartmut Grote, and Yuta Michimura for discussions of the optical configuration. We thank Henning Vahlbruch and Moritz Mehmet for discussions of sources of squeezed light. We also thank members of the "QI" consortium Katherine Dooley, Stuart Reid, Animesh Datta, Robert Hadfield, Dmitry Morozov, and Vincent Boyer for useful discussions of the proposed experiment. D. M. and H. M. acknowledge the support of the Institute for Gravitational Wave Astronomy at University of Birmingham. H. M. is supported by UK STFC Ernest Rutherford Fellowship (Grant No. ST/M005844/11).

[1] E. Aprile *et al.* (XENON Collaboration), Eur. Phys. J. C **77**, 881 (2017).
[2] D. Akerib *et al.*, Nucl. Instrum. Methods Phys. Res., Sect. A **704**, 111 (2013).
[3] H. Zhang *et al.*, Sci. China Phys. Mech. Astron. **62**, 31011 (2018).
[4] L. Baudis, A. Ferella, A. Kish, A. Manalaysay, T. M. Undagoitia, and M. Schumann, J. Cosmol. Astropart. Phys. 01 (2014) 044.
[5] A. Canepa, Rev. Phys. **4**, 100033 (2019).
[6] R. D. Peccei and H. R. Quinn, Phys. Rev. Lett. **38**, 1440 (1977).
[7] P. W. Graham and S. Rajendran, Phys. Rev. D **88**, 035023 (2013).
[8] A. Ringwald, Phys. Dark Universe **1**, 116 (2012).
[9] A. Ringwald, J. Phys. Conf. Ser. **485**, 012013 (2014).
[10] M. Farina, D. Pappadopulo, F. Rompineve, and A. Tesi, J. High Energy Phys. 1 (2017) 095.
[11] P. Svrcek and E. Witten, J. High Energy Phys. 06 (2006) 051.
[12] S. Weinberg, Phys. Rev. Lett. **40**, 223 (1978).
[13] M. Dine, W. Fischler, and M. Srednicki, Phys. Lett. B **104**, 199 (1981).
[14] D. Budker, P. W. Graham, M. Ledbetter, S. Rajendran, and A. O. Sushkov, Phys. Rev. X **4**, 021030 (2014).
[15] W. DeRocco and A. Hook, Phys. Rev. D **98**, 035021 (2018).
[16] I. Obata, T. Fujita, and Y. Michimura, Phys. Rev. Lett. **121**, 161301 (2018).
[17] H. Liu, B. D. Elwood, M. Evans, and J. Thaler, Phys. Rev. D **100**, 023548 (2019).
[18] LIGO Scientific Collaboration, Classical Quantum Gravity **32**, 074001 (2015).
[19] F. Acernese, M. Agathos, K. Agatsuma, D. Aisa, N. Allemandou, A. Allocca, J. Amarni, P. Astone, G. Balestri *et al.*, Classical Quantum Gravity **32**, 024001 (2015).
[20] LIGO Scientific and Virgo Collaborations, Phys. Rev. Lett. **116**, 061102 (2016).
[21] LIGO Scientific and Virgo Collaborations, Phys. Rev. Lett. **116**, 241103 (2016).
[22] LIGO Scientific and Virgo Collaborations, Phys. Rev. Lett. **118**, 221101 (2017).
[23] Y. Kahn, B. R. Safdi, and J. Thaler, Phys. Rev. Lett. **117**, 141801 (2016).
[24] J. L. Ouellet, C. P. Salemi, J. W. Foster, R. Henning, Z. Bogorad, J. M. Conrad, J. A. Formaggio, Y. Kahn, J. Minervini, A. Radovinsky, N. L. Rodd, B. R. Safdi, J. Thaler, D. Winklehner, and L. Winslow, Phys. Rev. Lett. **122**, 121802 (2019).
[25] K. Nagano, T. Fujita, Y. Michimura, and I. Obata, Phys. Rev. Lett. **123**, 111301 (2019).
[26] H. Miao, Y. Ma, C. Zhao, and Y. Chen, Phys. Rev. Lett. **115**, 211104 (2015).
[27] H. Miao, H. Yang, and D. Martynov, Phys. Rev. D **98**, 044044 (2018).
[28] LIGO Scientific Collaboration, Nat. Phys. **7**, 962 (2011).
[29] LIGO Scientific Collaboration, Nat. Photonics **7**, 613 (2013).
[30] M. Punturo, M. Abernathy, F. Acernese, B. Allen, N. Andersson, K. Arun, F. Barone, B. Barr *et al.*, Classical Quantum Gravity **27**, 194002 (2010).
[31] LIGO Scientific Collaboration, Classical Quantum Gravity **34**, 044001 (2017).
[32] M. Ivanov, Y. Kovalev, M. Lister, A. Panin, A. Pushkarev, T. Savolainen, and S. Troitsky, J. Cosmol. Astropart. Phys. 02 (2019) 059.
[33] E. D. Black, Am. J. Phys. **69**, 79 (2001).
[34] A. Staley *et al.*, Classical Quantum Gravity **31**, 245010 (2014).
[35] D. V. Martynov, E. D. Hall, B. P. Abbott *et al.*, Phys. Rev. D **93**, 112004 (2016).
[36] P. F. Cohadon, A. Heidmann, and M. Pinard, Phys. Rev. Lett. **83**, 3174 (1999).
[37] T. Corbitt, C. Wipf, T. Bodiya, D. Ottaway, D. Sigg, N. Smith, S. Whitcomb, and N. Mavalvala, Phys. Rev. Lett. **99**, 160801 (2007).
[38] T. P. Purdy, K. E. Grutter, K. Srinivasan, and J. M. Taylor, Science **356**, 1265 (2017).
[39] V. Sudhir, R. Schilling, S. A. Fedorov, H. Schütz, D. J. Wilson, and T. J. Kippenberg, Phys. Rev. X **7**, 031055 (2017).
[40] D. V. Martynov *et al.* (LSC Instrument Authors), Phys. Rev. A **95**, 043831 (2017).

[41] R. B. Hurst, G. E. Stedman, K. U. Schreiber, R. J. Thirkettle, R. D. Graham, N. Rabeendran, and J.-P. R. Wells, J. Appl. Phys. **105**, 113115 (2009).
[42] K. U. Schreiber, T. Klügel, J.-P. R. Wells, R. B. Hurst, and A. Gebauer, Phys. Rev. Lett. **107**, 173904 (2011).
[43] J. Belfi, N. Beverini, F. Bosi, G. Carelli, A. Di Virgilio, D. Kolker, E. Maccioni, A. Ortolan, R. Passaquieti, and F. Stefani, J. Seismol. **16**, 757 (2012).
[44] W. Z. Korth, A. Heptonstall, E. D. Hall, K. Arai, E. K. Gustafson, and R. X. Adhikari, Classical Quantum Gravity **33**, 035004 (2016).
[45] D. Martynov, N. Brown, E. Nolasco-Martinez, and M. Evans, Opt. Lett. **44**, 1584 (2019).
[46] M. Tse *et al.*, Phys. Rev. Lett. **123**, 231107 (2019).
[47] F. Acernese *et al.* (Virgo Collaboration), Phys. Rev. Lett. **123**, 231108 (2019).
[48] D. Martynov, Lock acquisition and sensitivity analysis of advanced LIGO interferometers, Ph.D. Thesis, Caltech, 2015.
[49] S. Gras, H. Yu, W. Yam, D. Martynov, and M. Evans, Phys. Rev. D **95**, 022001 (2017).
[50] B. Schumaker and C. Caves, Phys. Rev. A **31** (1985).
[51] Y. Chen, J. Phys. B **46**, 104001 (2013).
[52] H. Vahlbruch, M. Mehmet, K. Danzmann, and R. Schnabel, Phys. Rev. Lett. **117**, 110801 (2016).
[53] S. T. Pradyumna, E. Losero, I. Ruo-Berchera, P. Traina, M. Zucco, C. S. Jacobsen, U. L. Andersen, I. P. Degiovanni, M. Genovese, and T. Gehring, arXiv:1810.13386.
[54] M. Mehmet and H. Vahlbruch, Classical Quantum Gravity **36**, 015014 (2018).
[55] S. Chaudhuri, K. Irwin, P. W. Graham, and J. Mardon, arXiv:1803.01627.
[56] Y. Kahn, B. R. Safdi, and J. Thaler, Phys. Rev. Lett. **117**, 141801 (2016).
[57] V. Anastassopoulos *et al.* (CAST Collaboration), Nat. Phys. **13**, 584 (2017).
[58] R. Bähre, B. Döbrich, J. Dreyling-Eschweiler, S. Ghazaryan, R. Hodajerdi, D. Horns, F. Januschek, E. A. Knabbe, A. Lindner, D. Notz, A. Ringwald, J. E. von Seggern, R. Stromhagen, D. Trines, and B. Willke, J. Instrum. **8**, T09001 (2013).